Published in final edited form as:
Curr Biol. 2011 December 6; 21(23): 1960–1967. doi:10.1016/j.cub.2011.10.050.

A $G\alpha_q$ - Ca^{2+} signaling pathway promotes actin-mediated epidermal wound closure in *C. elegans*

Suhong Xu and **Andrew D. Chisholm***
Division of Biological Sciences, Section of Cell and Developmental Biology, University of California San Diego, 9500 Gilman Drive, La Jolla, CA 92093

Summary

Background—Repair of skin wounds is essential for animals to survive in a harsh environment, yet the signaling pathways initiating wound repair in vivo remain little understood. In *C. elegans* a p38 MAPK cascade promotes innate immune responses to wounding, but is not required for other aspects of wound healing. We therefore set out to identify additional wound response pathways in *C. elegans* epidermis.

Results—We show here that wounding the adult *C. elegans* skin triggers a rapid and sustained rise in epidermal Ca^{2+} that is critical for survival after wounding. The wound-triggered rise in Ca^{2+} requires the epidermal TRPM channel GTL-2 and IP_3R-stimulated release from internal stores. We identify an epidermal signal transduction pathway that includes the $G\alpha_q$ EGL-30 and its effector PLCβ EGL-8. Loss of function in this pathway impairs survival after wounding. The $G\alpha_q$-Ca^{2+} pathway is not required for known innate immune responses to wounding but instead promotes actin-dependent wound closure. Wound closure requires the Cdc42 small GTPase and Arp2/3 dependent actin polymerization, and is negatively regulated by Rho and non-muscle myosin. Finally, we show that the death-associated protein kinase DAPK-1 acts as a negative regulator of wound closure.

Conclusions—Skin wounding in *C. elegans* triggers a Ca^{2+}-dependent signaling cascade that promotes wound closure, in parallel to the innate immune response to damage. Wound closure requires actin polymerization and is negatively regulated by non-muscle myosin.

Keywords

laser; barrier epithelium; GCaMP; TRP channel; DAP kinase; innate immunity; actin polymerization; nonmuscle myosin; Cdc42; Rho GTPase

Introduction

All organisms must repair damage caused by mechanical injury or environmental pathogens. The skin in particular exhibits a complex sequence of wound healing processes [1]. Understanding the molecular basis of wound healing is of increasing relevance to human health as chronic or non-healing wounds become more common in the elderly or in diabetic individuals [2]. Several vertebrate and invertebrate models are being explored for molecular

*To whom correspondence should be addressed: chisholm@ucsd.edu.

genetic analyses of wound healing [3–5]. Importantly, transcription factors involved in epidermal wound healing show evolutionary conservation [6, 7], suggesting mechanisms in wound healing could share significant similarity.

Despite extensive efforts in the analysis of wound healing, many questions remain open. It is not well understood how barrier epithelia detect damage, nor how the initial sensation of damage is transmitted to develop a coordinated wound healing response. Studies in Drosophila wound healing have highlighted the role of epidermal tyrosine kinases and ERK signaling in early wound responses [8, 9], whereas mammalian wound responses appear to be initiated by a variety of growth factors and cytokines [10].

The epidermis of the nematode *C. elegans* is a simple barrier epithelium that generates an external cuticle. The nematode body is under hydrostatic pressure, so puncture wounds can be fatal if not repaired. Such wounds may be common in nature, where nematodes encounter damaging substrates and cuticle-puncturing pathogens [11, 12]. Needle or laser wounding of the epidermis triggers a p38 MAPK/PMK-1 cascade that activates transcription of antimicrobial peptide genes [13]. This innate immune response defends against opportunistic infection at wounds, as p38 MAPK mutants display reduced survival after wounding [14]. However, the p38 MAPK cascade is not required for other wound repair processes such as scar formation [14].

To address how other aspects of *C. elegans* wound healing are activated we have examined other known wound-triggered pathways. Ca^{2+} is important for embryonic wound healing [15] and in wound responses of single cells [16]. However the *in vivo* role of Ca^{2+} signals in repair of mature barrier epithelia has been less clear. We show here that Ca^{2+} signals are critical for *C. elegans* wound healing, acting in parallel to innate immune response pathways to promote actin rearrangement during wound closure. Unlike embryonic or single-cell wounds, which typically involve actomyosin purse-string based contractility [17], we find that wounds in the adult *C. elegans* skin close by an actin polymerization based mechanism negatively regulated by non-muscle myosin.

Results

Wounding triggers a rapid and sustained rise in epidermal Ca^{2+}

To visualize Ca^{2+} dynamics in the epidermis after wounding we expressed the Ca^{2+} sensor GCaMP3 [18] under the control of epidermal-specific promoters (see Experimental Procedures; Table S1). The adult *C. elegans* epidermis consists of seam cells and multinucleate syncytial cells, of which hyp7 is the largest. Needle wounding of the syncytial hyp7 epidermis in late larvae or adults triggered increases in epidermal GCaMP fluorescence that spread from the site of injury to approximately 1/3 the length of the animal (Movie S1; Figure 1A). To quantitate wound-triggered Ca^{2+} dynamics we performed localized laser wounding and imaged epidermal GCaMP using spinning-disk microscopy (Movie S2: Figure 1B,C). Laser wounding triggered increases in GCaMP fluorescence similar to those seen after needle wounding; GCaMP waves traveled at 25.6 ± 2 μm s^{-1} (Figure S1A), a speed consistent with propagation via Ca^{2+}-induced Ca^{2+} release from internal stores. Thereafter, elevated GCaMP fluorescence underwent small global oscillations but was otherwise stable, and typically persisted for > 1 h before declining (Movie S3; Figure 1D).

To test whether release from internal stores contributed to the epidermal Ca^{2+} wave we tested the IP_3 receptor ITR-1. *itr-1(jc5cs)* mutants displayed significantly reduced epidermal GCaMP responses to injury (Figure 1E,F). To reduce IP_3 signaling specifically in the epidermis we overexpressed N-terminal IP_3 binding domains ('IP_3 sponges') [19].

Expression of IP_3 sponges in the adult epidermis reduced both baseline and wound-induced increase in GCaMP fluorescence (Figure S1B,C), indicating that wounding triggers Ca^{2+} release from internal stores in the epidermis.

An epidermal TRPM channel is required for Ca^{2+} responses

Release of Ca^{2+} from internal stores could be triggered by an initial Ca^{2+} influx across the epidermal cell membrane or by other signals that activate the IP_3R. To define the sources of epidermal Ca^{2+} we screened known Ca^{2+} channels and Ca^{2+} signaling components (Table S2). *C. elegans* encodes ~100 Ca^{2+} channel subunits, including 17 divalent cation channels in the TRP class [20]. Several TRP channels are expressed in the epidermis, including the TRPM-family channel GTL-2 [21]. Of 11 TRP channels tested, only GTL-2 was required for normal epidermal Ca^{2+} responses (Figure 2A,B). Epidermal expression of GTL-2 rescued *gtl-2* Ca^{2+} defects (Figure 2B), whereas muscle- or neuron-specific expression did not rescue (not shown), suggesting GTL-2 can act cell-autonomously in epidermal Ca^{2+} homeostasis. GTL-2 is localized to the plasma membrane in the epidermis [21] suggesting GTL-2 may affect initial influx of Ca^{2+} after wounding rather than subsequent calcium-induced Ca^{2+} release.

Epidermal Ca^{2+} responses are required for survival of wounding

To address the importance of Ca^{2+} and GTL-2 in wound healing we analyzed survival post-wounding. We measured survival 24 h after needle wounding, a time when >90% of wounded wild-type animals are healthy [14]. *gtl-2* mutants showed drastically reduced survival post wounding, a phenotype rescued by epidermal expression of GTL-2, suggesting epidermal GTL-2 is required for survival after wounding (Figure 2C). Expression of IP_3 sponges in the epidermis caused smaller decreases in survival, consistent with their partial reduction in epidermal Ca^{2+} (Figure S1D). Loss of function in other TRPM family members GON-2 or GTL-1 can compensate for loss of GTL-2 function via systemic ion homeostasis [21, 22], and indeed *gtl-2 gon-2* or *gtl-2 gtl-1* double mutants showed restored viability after wounding (Figure S2B). These observations further support the model that GTL-2 contributes to epidermal Ca^{2+} homeostasis required for wound responses.

Reduced survival after wounding could reflect poor overall health rather than a defect in wound repair. To address whether developmental defects might account for reduced survival after wounding we used tissue- and stage-specific RNAi to reduce gene function only in the adult epidermis (see Experimental Procedures). Adult epidermal-specific RNAi of genes acting in the epidermal innate immune response, including the Toll/Interleukin receptor adaptor domain gene *tir-1* [23], reduced post-wound survival (Figure 2F), indicating effective gene knockdown in this strain. Adult epidermal-specific RNAi of Ca^{2+} signaling genes, including *itr-1* and *gtl-2*, significantly reduced post-wound survival (Figure 2F), confirming that ITR-1 and GTL-2 are required cell-autonomously for survival after epidermal wounding.

$G\alpha_q$ signaling is required for the epidermal Ca^{2+} response to wounding

Among genes required for normal Ca^{2+} levels in the epidermis we identified *egl-8*, which encodes phospholipase Cβ and *egl-30*, encoding the regulatory $G\alpha_q$ protein for EGL-8. *egl-8* and *egl-30* mutants both displayed reduced epidermal Ca^{2+} (Figure 2D, S2A) and impaired survival post-wounding (Figure 2E). *egl-8* null mutants did not enhance *gtl-2(lf)* survival phenotypes (Figure 2E), suggesting *egl-8* and *gtl-2* act in a common pathway. *egl-30* null mutants arrest during larval development, precluding firm conclusions from double mutants. However a gain of function mutation, *egl-30(js126)* significantly suppressed survival defects of *gtl-2(lf)* mutants, consistent with EGL-30 acting downstream or in parallel to GTL-2. As

PLCβ generates IP_3 in response to GPCR signals, these results suggest EGL-30 and PLCβ promote epidermal Ca^{2+} release via ITR-1 after wounding.

EGL-30 is expressed in many tissues, including the epidermis [24], whereas EGL-8 expression has been predominantly observed in neurons. We found that epidermal-specific RNAi of *egl-8* or *egl-30* significantly reduced post-wounding survival without affecting other behaviors such as egg-laying (Figure 2F; not shown). Conversely, epidermal-specific expression of EGL-8 was sufficient to rescue post-wound survival defects of *egl-8* mutants, but did not rescue their Egl phenotypes (not shown). We conclude the EGL-30/EGL-8 pathway functions within the epidermis to promote wound responses.

Ca^{2+} signals are not involved in the known innate immune responses to wounding

Sterile wounding activates an epidermal TIR-1/PMK-1 p38 MAPK cascade that induces epidermal expression of antimicrobial peptides (AMPs) such as *nlp-29* [13]. Wounding also induces p38-independent transcription of caenacin-type (*cnc*) AMPs via the SMA-6 TGFβ receptor [25]. We tested whether Ca^{2+} signaling might intersect with these pathways and found that loss of function in *gtl-2* or *egl-30* had no effect on induction of *nlp-29* or *nlp-30* (Figure 3A,B). *egl-8* null mutants also displayed normal AMP induction, consistent with previous results on *egl-8(n488)* [26]. *gtl-2* and *egl-30* mutants also showed normal induction of *cnc-1* and *cnc-2* after wounding (Figure 3B). These findings suggest $G\alpha_q/Ca^{2+}$ signals act in parallel to immune responses to wounding. Conversely, loss of function in the TIR-1/PMK-1 pathway or in $G\alpha_{12}$/GPA-12 did not affect epidermal Ca^{2+} (Figure S3A,B). Double mutants between *gtl-2* or *egl-8* and *tir-1* or *pmk-1* displayed additive or synergistic reductions in survival after wounding (Figure 3C). Taken together these results suggest that epidermal Ca^{2+} and innate immune responses act in parallel to promote survival after wounding.

Ca^{2+} signals trigger formation of actin rings at wounds

We next asked whether the need for Ca^{2+} signaling in survival of wounding reflected defects in specific repair processes. Healing of adult wounds typically involves cell proliferation, migration and re-epithelialization by cell crawling, and remodeling of ECM. In contrast, wound closure in embryonic epithelia is characterized by contractile actomyosin cables (‘purse-strings’) [27, 28]. Further, actin [29]cable formation in *Xenopus* oocyte wound closure is Ca^{2+}-dependent [30]. We therefore focused on whether Ca^{2+} signals promoted cytoskeletal dynamics in wound closure. To visualize the epidermal actin cytoskeleton we expressed the F-actin marker GFP-moesin [31] in the epidermis. GFP-moesin distribution in the unwounded epidermis was diffuse (Figure 4A). Within minutes of needle wounding a dense ring of filamentous GFP indicative of actin filaments formed at the site of damage (Movie S4; Figure 4A). In most cases the actin ring gradually closed over the next 1–2 h; a minority failed to close over this time period, possibly reflecting variability in needle wounding or in closure dynamics. After 24 h the actin rings were completely closed (Figure 4B), and colocalized with autofluorescent scar material [13]. These findings suggest that *C. elegans* adult wound closure involves a dynamic rearrangement of the actin cytoskeleton.

To quantitate the dynamics of actin during wound closure we used line scans of confocal images to measure the GFP-moesin ring diameter at 1 h after wounding, a time intermediate in the closure process (Figure 4C,D). We first tested whether Ca^{2+} signals promote closure by incubating wounded worms in Ca^{2+} chelators such as BAPTA-AM, and found that these treatments severely compromised actin ring formation (Figure 4C). Incubation in Ca^{2+} chelators also reduced survival post-wounding (Figure S1E). *gtl-2* mutants displayed reduced actin accumulation after wounding, and impaired closure of actin rings (Figure 4C,D; Movie S4). Incubation of *gtl-2* mutants in media containing increased external Ca^{2+}

significantly restored closure (Figure 4C,D), suggesting the closure defects of *gtl-2* mutants result from reduced epidermal Ca^{2+}. Conversely, mutants defective in innate immune responses (*tir-1, pmk-1*) displayed normal actin ring formation (Figure S3C). The reduced survival of immunocompromised mutants such as *tir-1* can be partly suppressed by incubation with antibiotics or DNA replication blockers such as FUDR [14]. In contrast, impaired survival of *gtl-2* or *egl-8* mutants was not suppressed by FUDR (Figure S2C), consistent with a defect in physical closure of wounds.

Wound closure involves local actin polymerization and is inhibited by non-muscle myosin

The dynamics of actin rings after wounding suggest wound closure involves the actin cytoskeleton, but do not distinguish whether this is driven by actomyosin-based contractility or some other form of actin dynamics. Time-lapse analysis of actin wounding suggested at least two processes contribute to actin dynamics: first, recruitment of F-actin to the ring, and second, closure of the ring. To address the role of actin we first tested actin polymerization inhibitors. Incubation of animals in the actin polymerization inhibitor Latrunculin A (LatA) completely blocked recruitment of actin to wounds (Figure S4A) and significantly reduced post-wounding survival (Figure S4B), indicating that actin polymerization is essential for formation of actin rings.

We next used RNAi to test the roles of known regulators of actin polymerization, including Rho-family GTPases and a set of actin binding or nucleating proteins. Among small GTPases, Rho is required for actin cable formation in wound closure [32], whereas Cdc42 is essential for actin assembly and disassembly in several contexts, including filopodial protrusions [33]. We found that *cdc-42(RNAi)* abolished actin recruitment to wound sites, whereas loss of function in *rho-1* caused actin rings to close more rapidly than in the wild type. In contrast, loss of function in the Rac genes (*rac-2, ced-10, mig-2*) had little effect on actin recruitment or survival (not shown). Knockdown of the actin nucleation factors WSP-1/WASP or ARX-2/Arp2/3 complex reduced but did not abolish ring closure (Figure 5A,B); *arx-2(RNAi)* strongly reduced survival post-wounding (Figure 5C). Taken together these results suggest that Cdc42-dependent actin polymerization is important for wound closure and survival.

Finally, to test whether *C. elegans* wound closure required actomyosin contractility we reduced the function of non-muscle myosin. *C. elegans* encodes two non-muscle myosin heavy chains, NMY-1 and NMY-2, with partly redundant functions in epidermal development [34]. Unexpectedly, loss of function in either *nmy* gene significantly promoted actin ring closure (Figure 6A,B; Movie S5), as did RNAi of the epidermally expressed myosin light chain *mlc-4*. *nmy-2(RNAi)* did not enhance *nmy-1* mutant phenotypes (Figure 6B), suggesting the *nmy* genes may be non-redundant in wound closure. Knockdown of non-muscle myosin light chain *mlc-4*(RNAi) also promoted ring closure(Figure 6A,B). Inhibition of non-muscle-myosin did not affect post-wounding survival (not shown). Time-lapse analysis of actin dynamics in *nmy-1(sb115)* mutants (Movie S5) suggested that wound closure was accelerated after knockdown of non-muscle myosin. Taken together, these results suggest *C. elegans* adult epidermal wounds do not close by a ‘purse-string’ mechanism. Instead, local actin polymerization related to filopodial protrusions appears to be critical.

Loss of DAP kinase function accelerates wound closure and suppresses the effects of Ca^{2+} signaling mutants

The Ca^{2+}-calmodulin regulated kinase DAPK/DAPK-1 has been shown to negatively regulate epidermal innate immune responses to damage [14] and is a known regulator of non-muscle myosin [35]. We therefore tested whether DAPK/*dapk-1* might also negatively

regulate cytoskeletal dynamics in wound closure. In *dapk-1* single mutants GFP-moesin rings were smaller than in the wild type and closed more rapidly, paralleling the *rho-1* and *nmy-1* phenotypes (Movie S5). To address whether such mutations could overcome the effects of reduced Ca^{2+} signals we constructed double mutants between *dapk-1* and *gtl-2, egl-8,* and *egl-30*. We found that *gtl-2 dapk-1* double mutants displayed significantly faster ring closure than did *gtl-2* mutants (Figure 6A,B). *dapk-1* mutants displayed normal epidermal Ca^{2+} dynamics (not shown). Finally, the low post-wound survival of *egl-30, egl-8,* or *gtl-2* single and compound mutants was significantly suppressed by *dapk-1(lf)* (Figure 6C). These results support DAPK-1 acting as a negative regulator of wound closure dynamics, either downstream or in parallel to Ca^{2+} signals.

Discussion

In conclusion, we have identified a G-protein/Ca^{2+} based wound closure pathway in the adult *C. elegans* epidermis. Our results link single-cell and embryonic wound models to physiologically relevant outcomes in repair of a mature barrier epithelium. Previous work has shown epidermal immune responses to wounding and fungal infection depend on $G\alpha_{12}$/GPA-12 [26]. We find that $G\alpha_q$/EGL-30 and Ca^{2+} act in parallel to promote epidermal wound closure via actin polymerization (Figure 7A,B). Although the $G\alpha_q$-Ca^{2+} pathway described here is not required for upregulation of antimicrobial peptides after wounding, it could play other roles in antimicrobial defense. For example, $G\alpha_q$ and PLCβ regulate insulin secretion and PMK-1 in intestinal innate immunity in *C. elegans* [36]. Clearly, an important future goal is to identify the activators and effectors of $G\alpha_q$ in the epidermis.

Our analysis suggests at least two sources contribute to epidermal Ca^{2+}, possibly in sequence. The TRPM channel GTL-2 is important for epidermal Ca^{2+} responses, suggesting wounding triggers an influx of Ca^{2+} via GTL-2. As several studies indicate GTL-2 localizes to cell plasma membranes rather than internal compartments [21, 22], it might directly sense wound-triggered changes in membrane tension. Alternatively, like other mechanosensitive TRP channels, GTL-2 might be indirectly gated by GPCR signaling [37]. The mechanism of gating of GTL-2 remains an open question. The EGL-30/EGL-8 pathway may be activated by an initial GTL-2-dependent Ca^{2+} influx to trigger further ITR-1-dependent release of Ca^{2+} from intracellular stores. Mammalian epidermal cells express a variety of TRP channels, some of which are implicated in epidermal wound healing [38]. Indeed, application of TRPM agonists can promote barrier reformation after wounding [39], suggesting some roles of TRPM channels in wound healing may be conserved.

Our results suggest a model for how Ca^{2+} signals trigger wound closure in the adult *C. elegans* epidermis (Figure 7B). CDC-42 is essential for actin rings to form, consistent with findings that Cdc42 is important in Drosophila larval wound closure [29]. As Cdc42 is activated by Ca^{2+} after wounding in *Xenopus* oocytes [40], it may act downstream of the Ca^{2+} signal in the *C. elegans* epidermis. Why does actin accumulate locally at wound sites when the Ca^{2+} signal is delocalized? This may be explained if Ca^{2+} acts with a local signal, possibly generated by cellular ‘compartment mixing’ [41]. In contrast, Rho acts antagonistically to CDC-42 in *C. elegans* wound responses. Rho and CDC-42 might directly antagonize, as in *Xenopus* oocyte wounding [42]. Alternatively, the enhanced closure seen after inhibition of Rho or non-muscle myosin might be an indirect consequence of reduced actin cable formation. Future studies should address whether and how Rho and CDC-42 are locally activated at wounds. Nevertheless, our results suggest that, unlike embryonic epithelia in which purse-string actomyosin contractility has a major role, wound closure in the adult *C. elegans* epidermis is driven by directed actin polymerization. The unexpected negative role of non-muscle myosin suggests actin cable formation may compete with actin polymerization in wound closure. *C. elegans* wound closure may more resemble that found

in other adult epithelia, in which closure is driven by filopodial protrusion at the epithelial leading edge [43]. Most of our wounds affect the large syncytial epidermal cell hyp7, distant from their contacts with other epidermal cells such as seam cells. We therefore believe that actin structures formed after wounding are predominantly generated by hyp7, although contributions from other epidermal cells have not yet been examined.

Death Associated Protein Kinase DAPK-1 is a negative regulator of the innate immune response to wounding [14]. As DAPK is regulated by Ca^{2+} [44], DAPK-1 is an excellent candidate to be regulated by Ca^{2+} signals reported here. The inhibitory role of DAPK-1 in closure, together with previous evidence that DAPK-1 inhibits the innate immune response to damage, indicate DAPK-1 acts as a coordinate negative regulator of wound responses. If this inhibitory role for DAPK is conserved, pharmacological inhibition of DAPK could be a promising avenue for acceleration of wound healing.

Experimental Procedures

C. elegans genetics

All strains were maintained at 20–22.5 °C on NGM agar plates with *E. coli* OP50 as food source. Strains were constructed using standard procedures, and genotypes confirmed by PCR or sequencing. Mutations used include: *gtl-2[n2618(lf), tm1463(0)]*, *egl-8[n488(dn), sa47(0)]*, *egl-30(n686, ad805, js126gf)*, *itr-1(jc5cs)*, *dapk-1(ju4, gk219)*, *rde-1(ne219)*, *pmk-1(km25)*, *tir-1(tm3036)*, *tpa-1(k501, k530)*, *gpa-12(pk322)*, *gon-2(q365)*, *gtl-1(dx171)*, *nmy-1(sb115)*. New transgenic strains are listed in Table S1.

Needle wounding, survival assay, and drug experiments

We wounded animals with single stabs of a microinjection needle to the posterior body 24 h after L4 stage, as described [13]. We transferred wounded animals to new plates and scored viability every 24 h; we defined death as failure to respond to touch. In some assays we prevented bacterial proliferation and egg-laying by transferring animals to plates containing 50 mg/mL FUDR immediately before wounding. Calcium chelators or Latrunculin A were dissolved in DMSO or M9 then diluted in M9. We incubated wounded worms in drug solution (containing *E. coli* OP50) and checked survival every 12 h; control animals were incubated in M9 or DMSO. In experiments where unwounded strains displayed similar survival 24 h after L4 we calculated normalized survival (fraction surviving 24 h after wounding)/(fraction surviving unwounded). To image GCaMP after needle wounding on plates we used a Zeiss Discovery V12 dissecting stereomicroscope and a Nikon DS Qi-1 monochrome camera.

Adult epidermal-specific RNAi

To knock down gene expression in the adult epidermis we expressed the wild type RDE-1 gene under the control of P*col-19* (*juIs346*) in an *rde-1(ne219)* mutant background. *rde-1* mutants are resistant to RNAi; as the *col-19* promoter is expressed only in late L4 and adult epidermis, transgenic animals are resistant to RNAi in all tissues except the adult epidermis. We transferred *rde-1; Pcol-19-RDE-1(juIs346)* as L1s to bacteria expressing appropriate dsRNA, wounded the animals as day 1 adults, and assayed survival after 24 h. Other (tissue-nonspecific) RNAi experiments were performed in a similar way, with animals grown from the L1 stage on RNAi bacteria and wounded as young adults. Feeding RNAi clones were obtained from the Ahringer library and confirmed by sequencing, or made by PCR from cDNA or genomic templates; a complete list of RNAi clones is available on request.

Laser wounding and imaging

To analyze epidermal Ca^{2+} we wounded animals using femtosecond laser irradiation, essentially as described [45] except with 2 × 200 ms pulses. We imaged GCaMP fluorescence using spinning disk confocal microscopy, as described [45]. For short movies (<30 s) we acquired a single channel in burst mode; for longer time-lapse series we acquired two channels every 30–60 s. To measure peak $\Delta F/F_0$ we imaged 10 frames using a 100× objective (Zeiss Planapo, NA 1.46). We measured average fluorescence in ten equivalent regions of interest (ROI), five centered on the epidermal cell and five in the background. Baseline fluorescence (F_0) was obtained by averaging fluorescence in 5 ROIs in the epidermis then subtracting the average of 5 ROIs in the background before injury. GCaMP fluorescence was normalized to an internal control, P*col-19*-tdTomato; tdTomato or GFP levels did not change after wounding (Figure S1B). The change in fluorescence ΔF was expressed as the ratio of change with respect to the baseline $[(F_t-F_0)/F_0]$. To follow $\Delta F/F_0$ over time at different distances from the injury site we imaged using the 63× objective and drew 2 μm ROIs at intervals of 5 μm. As the GCaMP transient extended 10 μm from the injury site within 230 ms of wounding, we selected a 10 μm long ROI to compare initial $\Delta F/F_0$ between conditions.

To quantitate epidermal GFP-moesin (*juIs352*) we used confocal microscopy to acquire z-stacks (13 × 0.5 μm) of GFP-moesin rings after wounding. We generated maximum intensity projections of each z-stack. For each image we used 4 line scans (oriented at 45° to each other) over the GFP-moesin ring and defined actin ring diameter as the average peak to peak distance. In some conditions (e.g. BAPTA-AM, *gtl-2*) a significant fraction of animals did not assemble GFP-moesin rings after wounding; such animals were not included in quantitation. In cases where the actin ring had closed by 1 h we defined the diameter as 0. In embryonic epidermis GFP–moesin localized to circumferential bundles (not shown), consistent with known distribution of F-actin.

Statistical analysis

All statistical analyses used GraphPad Prism (La Jolla, CA). Two-way comparisons used the Student t-test, Mann-Whitney test, or the Fisher exact test for proportions.

Highlights

- Wounding the *C. elegans* skin triggers epidermal Ca^{2+} responses
- Wound triggered Ca^{2+} responses require the TRPM channel GTL-2 and PLCβ/Gα_q signals.
- Ca^{2+} responses regulate actin polymerization dependent wound closure
- DAPK is a coordinate negative regulator of wound responses

Supplementary Material

Refer to Web version on PubMed Central for supplementary material.

Acknowledgments

We thank Amy Tong for initial work on the epidermal calcium sensor, Tiffany Hsiao for help with transgene integration and mapping, Zilu Wu for assistance with the femtosecond laser, Claudiu Giurumescu for help with confocal imaging, and Anindya Ghosh-Roy for constructs and advice on GCaMP imaging. We thank Loren Looger for GCaMP3, Arshad Desai and Fabio Piano for the moesin clone, Emily Troemel for use of her real-time PCR machine, and Tamara Stawicki and Yishi Jin for sharing information and reagents prior to publication. We thank

Yishi Jin, Bill McGinnis, Karen Oegema, Emily Troemel, Nathalie Pujol, Jonathan Ewbank, and members of the Jin and Chisholm labs for discussions and comments on this manuscript. Supported by NIH R01 GM54657 to A.C.

References

1. Gurtner GC, Werner S, Barrandon Y, Longaker MT. Wound repair and regeneration. Nature. 2008; 453:314–321. [PubMed: 18480812]
2. Sen CK, Gordillo GM, Roy S, Kirsner R, Lambert L, Hunt TK, Gottrup F, Gurtner GC, Longaker MT. Human skin wounds: a major and snowballing threat to public health and the economy. Wound Repair Regen. 2009; 17:763–771. [PubMed: 19903300]
3. Martin P. Wound healing--aiming for perfect skin regeneration. Science. 1997; 276:75–81. [PubMed: 9082989]
4. Schafer M, Werner S. Transcriptional control of wound repair. Annu Rev Cell Dev Biol. 2007; 23:69–92. [PubMed: 17474876]
5. Galko MJ, Krasnow MA. Cellular and genetic analysis of wound healing in *Drosophila* larvae. PLoS Biol. 2004; 2:E239. [PubMed: 15269788]
6. Mace KA, Pearson JC, McGinnis W. An epidermal barrier wound repair pathway in Drosophila is mediated by grainy head. Science. 2005; 308:381–385. [PubMed: 15831751]
7. Ting SB, Caddy J, Hislop N, Wilanowski T, Auden A, Zhao LL, Ellis S, Kaur P, Uchida Y, Holleran WM, et al. A homolog of Drosophila grainy head is essential for epidermal integrity in mice. Science. 2005; 308:411–413. [PubMed: 15831758]
8. Wang S, Tsarouhas V, Xylourgidis N, Sabri N, Tiklova K, Nautiyal N, Gallio M, Samakovlis C. The tyrosine kinase Stitcher activates Grainy head and epidermal wound healing in Drosophila. Nat Cell Biol. 2009; 11:890–895. [PubMed: 19525935]
9. Wu Y, Brock AR, Wang Y, Fujitani K, Ueda R, Galko MJ. A blood-borne PDGF/VEGF-like ligand initiates wound-induced epidermal cell migration in Drosophila larvae. Curr Biol. 2009; 19:1473–1477. [PubMed: 19646875]
10. Werner S, Grose R. Regulation of wound healing by growth factors and cytokines. Physiol Rev. 2003; 83:835–870. [PubMed: 12843410]
11. Luo H, Liu Y, Fang L, Li X, Tang N, Zhang K. *Coprinus comatus* damages nematode cuticles mechanically with spiny balls and produces potent toxins to immobilize nematodes. Appl Environ Microbiol. 2007; 73:3916–3923. [PubMed: 17449690]
12. Glockling SL, Beakes GW. An ultrastructural study of sporidium formation during infection of a rhabditid nematode by large gun cells of *Haptoglossa heteromorpha*. J Invertebr Pathol. 2000; 76:208–215. [PubMed: 11023749]
13. Pujol N, Cypowyj S, Ziegler K, Millet A, Astrain A, Goncharov A, Jin Y, Chisholm AD, Ewbank JJ. Distinct innate immune responses to infection and wounding in the *C. elegans* epidermis. Curr Biol. 2008; 18:481–489. [PubMed: 18394898]
14. Tong A, Lynn G, Ngo V, Wong D, Moseley SL, Ewbank JJ, Goncharov A, Wu YC, Pujol N, Chisholm AD. Negative regulation of *Caenorhabditis elegans* epidermal damage responses by death-associated protein kinase. Proc Natl Acad Sci U S A. 2009; 106:1457–1461. [PubMed: 19164535]
15. Stanisstreet M. Calcium and wound healing in *Xenopus* early embryos. J Embryol Exp Morphol. 1982; 67:195–205. [PubMed: 6806425]
16. McNeil PL, Steinhardt RA. Plasma membrane disruption: repair, prevention, adaptation. Annu Rev Cell Dev Biol. 2003; 19:697–731. [PubMed: 14570587]
17. Nodder S, Martin P. Wound healing in embryos: a review. Anat Embryol (Berl). 1997; 195:215–228. [PubMed: 9084820]
18. Tian L, Hires SA, Mao T, Huber D, Chiappe ME, Chalasani SH, Petreanu L, Akerboom J, McKinney SA, Schreiter ER, et al. Imaging neural activity in worms, flies and mice with improved GCaMP calcium indicators. Nat Methods. 2009; 6:875–881. [PubMed: 19898485]
19. Walker DS, Gower NJ, Ly S, Bradley GL, Baylis HA. Regulated disruption of inositol 1,4,5-trisphosphate signaling in *Caenorhabditis elegans* reveals new functions in feeding and embryogenesis. Mol Biol Cell. 2002; 13:1329–1337. [PubMed: 11950942]

20. Kahn-Kirby AH, Bargmann CI. TRP channels in *C elegans*. Annu Rev Physiol. 2006; 68:719–736. [PubMed: 16460289]
21. Stawicki T, Zhou K, Yochem J, Chen L, Jin Y. TRPM channels modulate epileptic-like convulsions via systemic ion homeostasis. Curr Biol. 2011; 21:883–888. [PubMed: 21549603]
22. Teramoto T, Sternick LA, Kage-Nakadai E, Sajjadi S, Siembida J, Mitani S, Iwasaki K, Lambie EJ. Magnesium excretion in *C elegans* requires the activity of the GTL-2 TRPM channel. PLoS One. 2010; 5:e9589. [PubMed: 20221407]
23. Couillault C, Pujol N, Reboul J, Sabatier L, Guichou JF, Kohara Y, Ewbank JJ. TLR-independent control of innate immunity in *Caenorhabditis elegans* by the TIR domain adaptor protein TIR-1, an ortholog of human SARM. Nat Immunol. 2004; 5:488–494. [PubMed: 15048112]
24. Bastiani CA, Gharib S, Simon MI, Sternberg PW. *Caenorhabditis elegans* Gαq regulates egg-laying behavior via a PLCβ-independent and serotonin-dependent signaling pathway and likely functions both in the nervous system and in muscle. Genetics. 2003; 165:1805–1822. [PubMed: 14704167]
25. Zugasti O, Ewbank JJ. Neuroimmune regulation of antimicrobial peptide expression by a noncanonical TGF-β signaling pathway in *Caenorhabditis elegans* epidermis. Nat Immunol. 2009; 10:249–256. [PubMed: 19198592]
26. Ziegler K, Kurz CL, Cypowyj S, Couillault C, Pophillat M, Pujol N, Ewbank JJ. Antifungal innate immunity in *C. elegans*: PKCδ links G protein signaling and a conserved p38 MAPK cascade. Cell Host Microbe. 2009; 5:341–352. [PubMed: 19380113]
27. Martin P, Lewis J. Actin cables and epidermal movement in embryonic wound healing. Nature. 1992; 360:179–183. [PubMed: 1436096]
28. Wood W, Jacinto A, Grose R, Woolner S, Gale J, Wilson C, Martin P. Wound healing recapitulates morphogenesis in *Drosophila* embryos. Nat Cell Biol. 2002; 4:907–912. [PubMed: 12402048]
29. Lesch C, Jo J, Wu Y, Fish GS, Galko MJ. A targeted UAS-RNAi screen in *Drosophila* larvae identifies wound closure genes regulating distinct cellular processes. Genetics. 2010; 186:943–957. [PubMed: 20813879]
30. Clark AG, Miller AL, Vaughan E, Yu HY, Penkert R, Bement WM. Integration of single and multicellular wound responses. Curr Biol. 2009; 19:1389–1395. [PubMed: 19631537]
31. Edwards KA, Demsky M, Montague RA, Weymouth N, Kiehart DP. GFP-moesin illuminates actin cytoskeleton dynamics in living tissue and demonstrates cell shape changes during morphogenesis in Drosophila. Dev Biol. 1997; 191:103–117. [PubMed: 9356175]
32. Brock J, Midwinter K, Lewis J, Martin P. Healing of incisional wounds in the embryonic chick wing bud: characterization of the actin purse-string and demonstration of a requirement for Rho activation. J Cell Biol. 1996; 135:1097–1107. [PubMed: 8922389]
33. Nobes CD, Hall A. Rho, rac, and cdc42 GTPases regulate the assembly of multimolecular focal complexes associated with actin stress fibers, lamellipodia, and filopodia. Cell. 1995; 81:53–62. [PubMed: 7536630]
34. Piekny AJ, Johnson JL, Cham GD, Mains PE. The *Caenorhabditis elegans* nonmuscle myosin genes *nmy-1* and *nmy-2* function as redundant components of the *let-502*/Rho-binding kinase and *mel-11*/myosin phosphatase pathway during embryonic morphogenesis. Development. 2003; 130:5695–5704. [PubMed: 14522875]
35. Bialik S, Bresnick AR, Kimchi A. DAP-kinase-mediated morphological changes are localization dependent and involve myosin-II phosphorylation. Cell Death Differ. 2004; 11:631–644. [PubMed: 15002035]
36. Kawli T, Wu C, Tan MW. Systemic and cell intrinsic roles of Gqα signaling in the regulation of innate immunity, oxidative stress, and longevity in *Caenorhabditis elegans*. Proc Natl Acad Sci U S A. 2010; 107:13788–13793. [PubMed: 20647387]
37. Christensen AP, Corey DP. TRP channels in mechanosensation: direct or indirect activation? Nat Rev Neurosci. 2007; 8:510–521. [PubMed: 17585304]
38. Yamada T, Ueda T, Ugawa S, Ishida Y, Imayasu M, Koyama S, Shimada S. Functional expression of transient receptor potential vanilloid 3 (TRPV3) in corneal epithelial cells: involvement in thermosensation and wound healing. Exp Eye Res. 2010; 90:121–129. [PubMed: 19793539]

39. Denda M, Tsutsumi M, Denda S. Topical application of TRPM8 agonists accelerates skin permeability barrier recovery and reduces epidermal proliferation induced by barrier insult: role of cold-sensitive TRP receptors in epidermal permeability barrier homoeostasis. Exp Dermatol. 2010; 19:791–795. [PubMed: 20636355]
40. Benink HA, Bement WM. Concentric zones of active RhoA and Cdc42 around single cell wounds. J Cell Biol. 2005; 168:429–439. [PubMed: 15684032]
41. Bement WM, Yu HY, Burkel BM, Vaughan EM, Clark AG. Rehabilitation and the single cell. Curr Opin Cell Biol. 2007; 19:95–100. [PubMed: 17174083]
42. Vaughan EM, Miller AL, Yu HY, Bement WM. Control of local Rho GTPase crosstalk by Abr. Curr Biol. 2011; 21:270–277. [PubMed: 21295482]
43. Sonnemann KJ, Bement WM. Wound Repair: Toward Understanding and Integration of Single-Cell and Multicellular Wound Responses. Annu Rev Cell Dev Biol. 2010; 27:237–263. [PubMed: 21721944]
44. Bialik S, Kimchi A. The death-associated protein kinases: structure, function, and beyond. Annu Rev Biochem. 2006; 75:189–210. [PubMed: 16756490]
45. Ghosh-Roy A, Wu Z, Goncharov A, Jin Y, Chisholm AD. Calcium and cyclic AMP promote axonal regeneration in *Caenorhabditis elegans* and require DLK-1 kinase. J Neurosci. 2010; 30:3175–3183. [PubMed: 20203177]

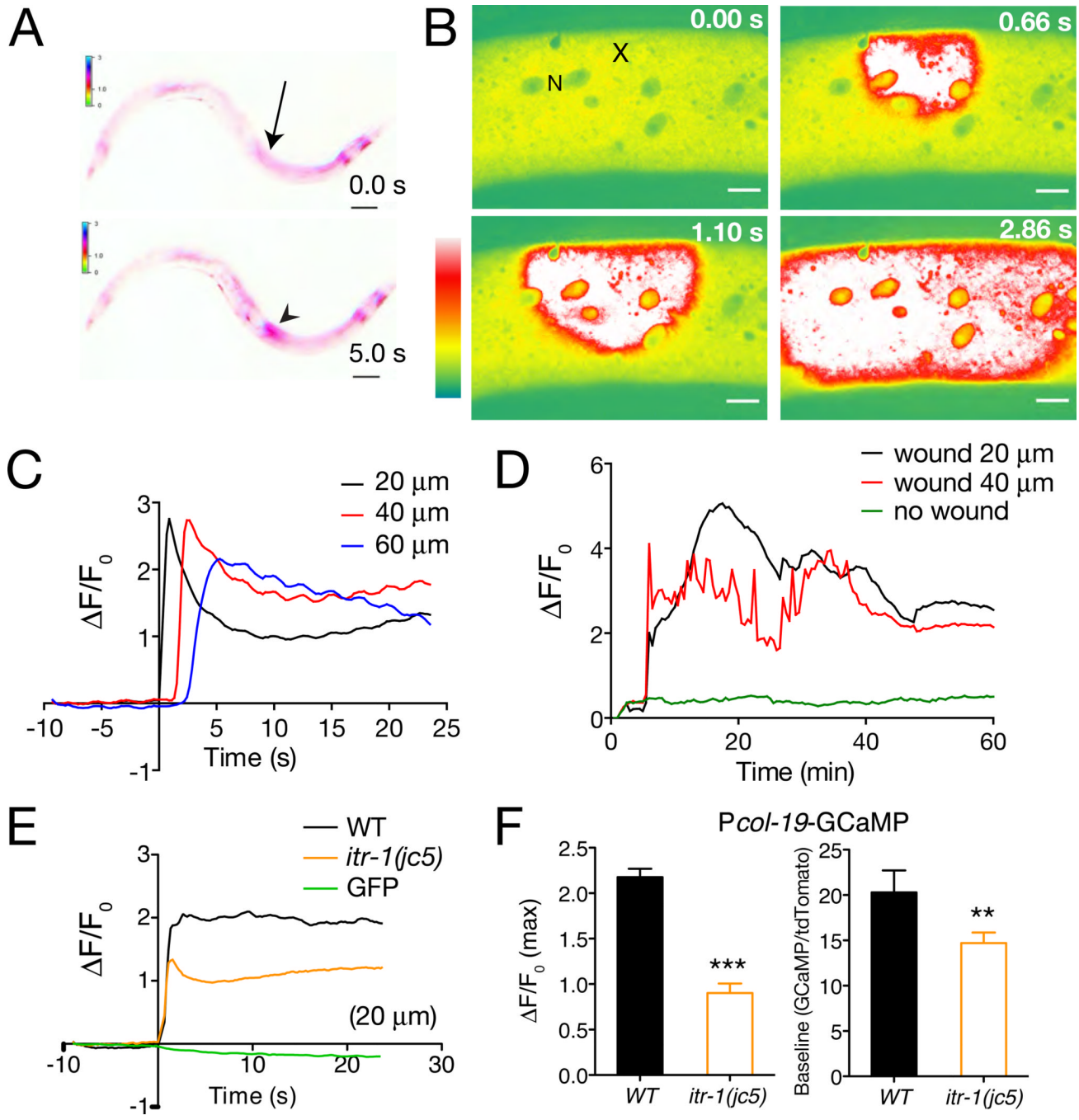

Figure 1. Wounding triggers an epidermal Ca^{2+} response

(A) Epidermal GCaMP induction after needle wounding; P*col-19*-GCaMP (*juIs319*). Site of wounding indicated by arrow; GCaMP fluorescence increase, arrowhead (see also Movie S1); inverted color scale. (B) Epidermal GCaMP fluorescence levels after femtosecond laser wounding. Lateral view of epidermis in mid-body; x, site of laser wound; N, epidermal nucleus. Spinning disk confocal, intensity code. See also Movie S2. (C) Quantitation of GCaMP $\Delta F/F_0$ at 20, 40, and 60 µm from wound site; representative trace. Note oscillations in GCaMP levels. (D) Prolonged elevation of epidermal GCaMP fluorescence after wounding; representative trace, from Movie S3 at positions 20 and 40 µm from wound site. Unwounded animals display minimal variation in GCaMP signals (green line). (E)

itr-1(jc5cs) mutants cultured at 15°C display reduced GCaMP $\Delta F/F_0$ compared to WT (average traces); wounding does not affect epidermal GFP fluorescence (green line, E). (F) *itr-1* mutants display reduced peak $\Delta F/F_0$ after wounding and reduced baseline GCaMP fluorescence, measured as ratio to epidermally expressed tdTomato. n > 20 per genotype Scales, 10 μm.

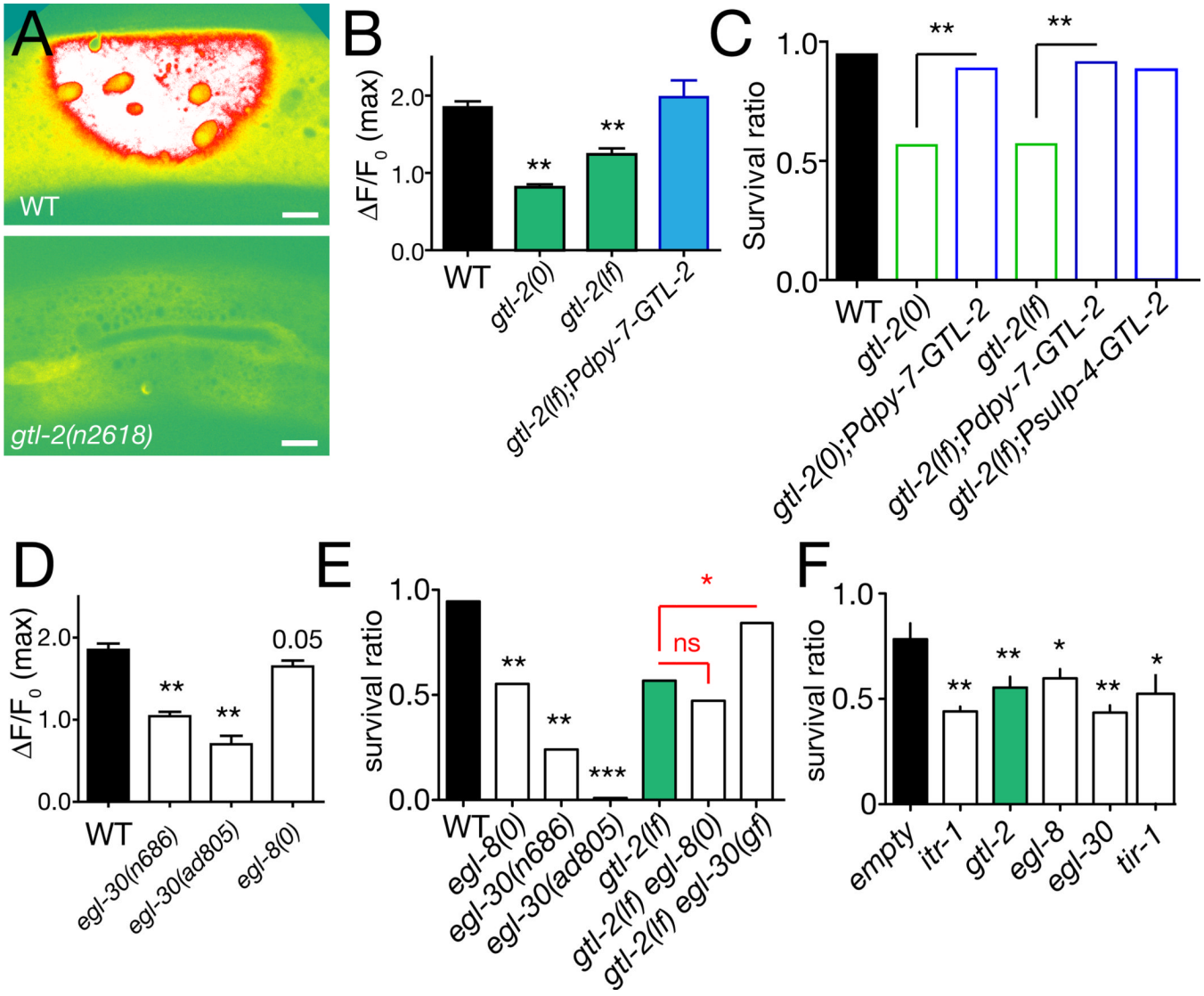

Figure 2. TRPM channel GTL-2 and Gαq/PLCβ signaling are required for epidermal Ca^{2+} responses and survival after wounding

(A) Epidermal Ca^{2+} responses to wounding are reduced in *gtl-2* mutants; imaged of P*col-19*-GCaMP(*juIs319*) (1 s after laser wound). (B) Quantitation of peak $\Delta F/F_0$ in *gtl-2(0)* null mutants (*tm1463*) and *gtl-2(lf)* partial loss of function *n2618* mutants; rescue by expression of GTL-2 under epidermal control (*juEx2893*). n > 30 per genotype. (C) *gtl-2* mutants display reduced survival after wounding; rescue by GTL-2::GFP expressed under control of epidermal (P*dpy-7*, *juEx2893*) or excretory system (P*sulp-4*, *juEx3216*) promoters. GTL-2::GFP signals are weak and do not interfere with GCaMP imaging. Survival ratio calculated as fraction of animals alive 24 h post wounding/number unwounded alive; n > 100 per genotype. (D) Partial loss of function in *egl-30* strongly reduces epidermal baseline Ca^{2+} and $\Delta F/F_0$; loss of function in *egl-8* reduces baseline GCaMP signal and has a small effect on $\Delta F/F_0$; n > 50 per genotype. (E) Reduced survival of *egl-8* and *egl-30* mutants post wounding; *egl-8(0) gtl-2(lf)* double mutants are not further enhanced; n > 500 per genotype. Improved survival of *gtl-2 egl-30(gf)* double mutants. (F) Epidermal-specific RNAi of *egl-8* and *egl-30* significantly reduces survival post-wounding, comparably to RNAi of *itr-1* or *gtl-2*; n > 200 per RNAi. All bar charts show mean ± SEM. Statistics, t test (B), Mann-

Whitney test (D, F), or Fisher exact test (C,E); ***, $P < 0.001$, **, $P < 0.01$; *, $P < 0.05$; ns, not significant.

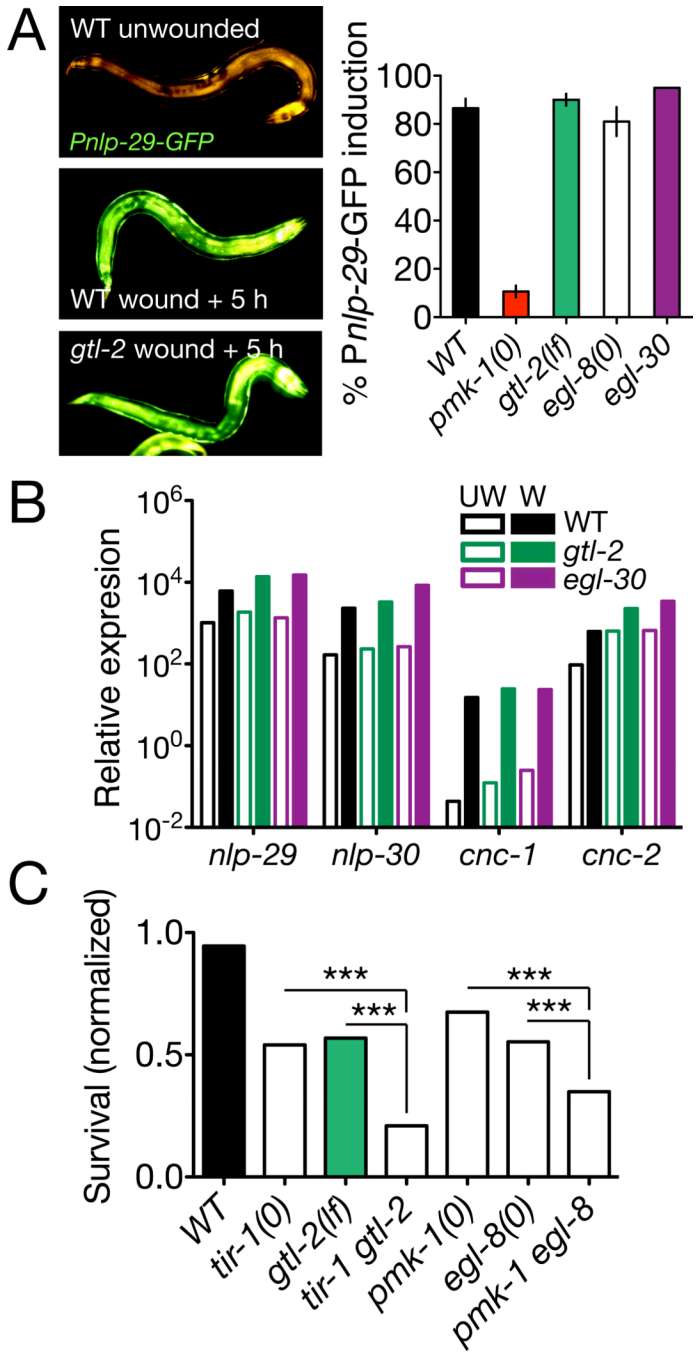

Figure 3. Epidermal Ca^{2+} signals act in parallel to known innate immune pathways

(A) Representative images (wild type (WT) unwounded, WT wounded + 5 h and *gtl-2* wounded + 5 h) and quantitation of P*nlp-29*-GFP(*frIs7*) induction after needle wounding; n > 100 per genotype. (B) *gtl-2(n2618)* and *egl-30(n686)* mutants displayed normal basal levels (UW, empty bars) and wound-induced levels (W, filled bars) of epidermal antimicrobial peptide transcripts; RNA extracted from ~50 animals 6 h after needle wounding. Expression levels are relative to *ama-1* in multiple quantitative RT-PCRs. (C) Loss of function in Ca^{2+} signaling genes and in innate immune response genes has additive or synergistic effects on post-wounding survival. n > 300 per genotype. Statistics, Fisher exact test.

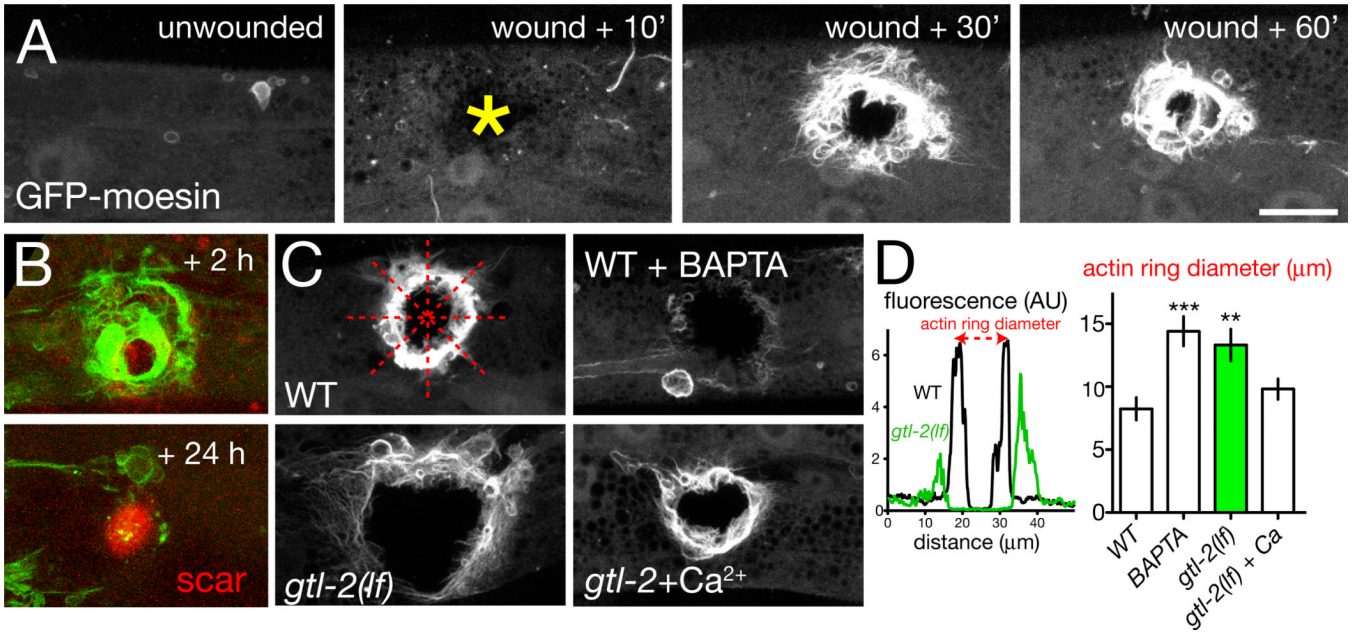

Figure 4. Wounding triggers Ca^{2+}-dependent formation of actin rings

(A) Epidermal needle wounds trigger formation of actin rings at the wound margin, visualized with P*col-19*-GFP-moesin (*juIs352*); frames from Movie S4. Scales in A–C, 10 μm. (B) In wild type animals actin rings close by 24 h; an autofluorescent scar (red channel) remains, marking the wound. (C,D) GFP intensity along line scans of representative WT and *gtl-2(n2618)* mutants; arbitrary units. Quantitation of actin ring diameter from line scans, n > 20 per genotype; 4 line scans per animal (dotted red lines in panel C, WT); Mann-Whitney test. Actin ring assembly and closure is inhibited by incubation in BAPTA-AM and in *gtl-2* mutants. In ~42% of BAPTA-treated animals and 29% of *gtl-2* mutants the GFP-moesin ring never forms; ring diameters were quantitated in remaining animals. The *gtl-2* actin closure defect is partly suppressed by incubation in buffer containing 2 mM Ca^{2+} (P = 0.05).

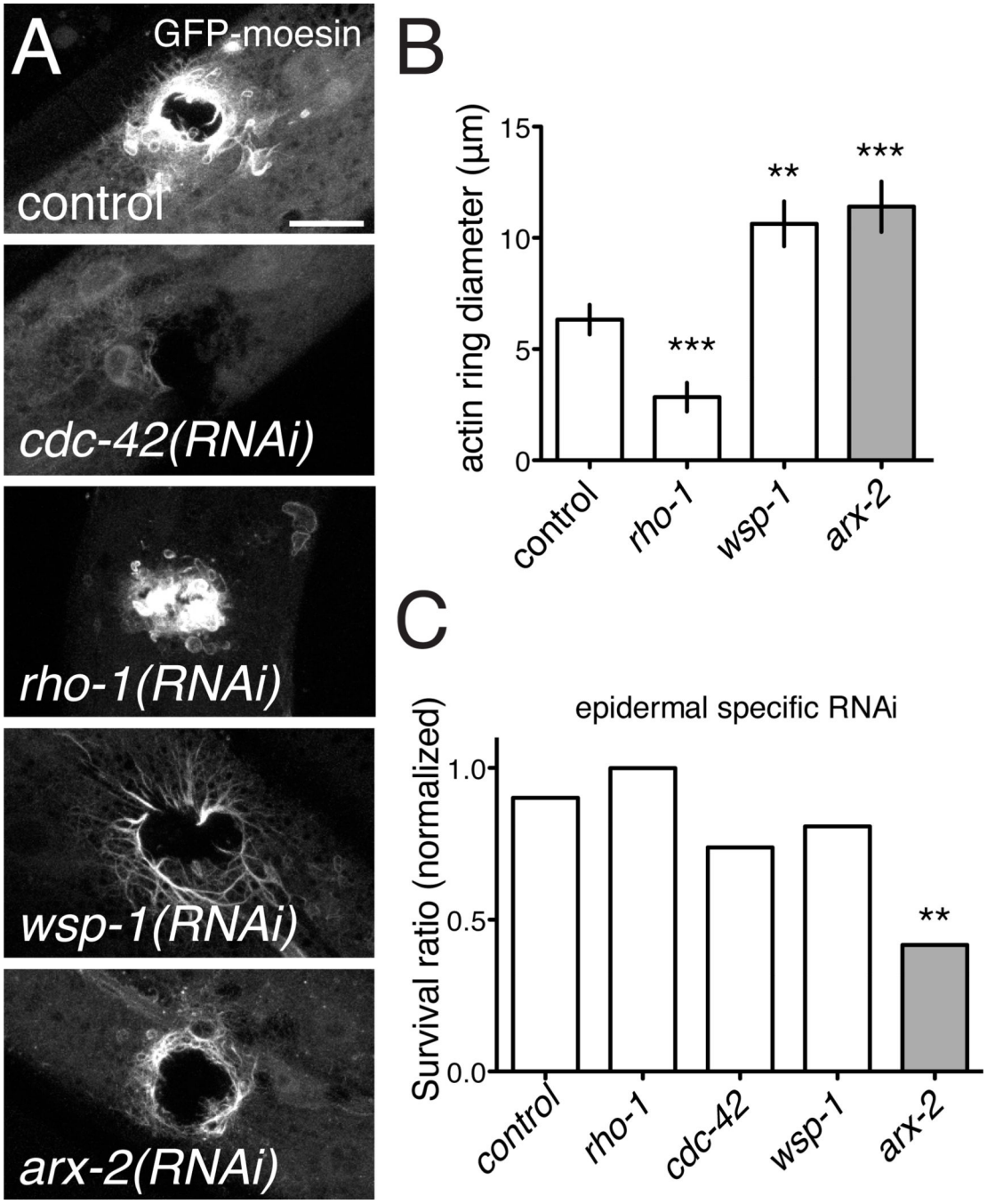

Figure 5. Wound closure requires actin polymerization factors and Cdc42, and is inhibited by Rho

(A,B) Ring formation is abolished in *cdc-42(RNAi)* animals and promoted in *rho-1(RNAi)* animals (control, L4440 empty vector). Of the three Rac genes, only *mig-2* showed a weak requirement for ring formation (not shown). Ring closure was reduced after RNAi for *wsp-1*/WASP and *arx-2*/Arp2/3. Scale, 10 μm (A). (C) Survival post-wounding is unaffected by *rho-1(RNAi)*, slightly impaired by *cdc-42(RNAi)*, and strongly reduced by *arx-2(RNAi)*. Statistics, t test (C) or Fisher exact test (B).

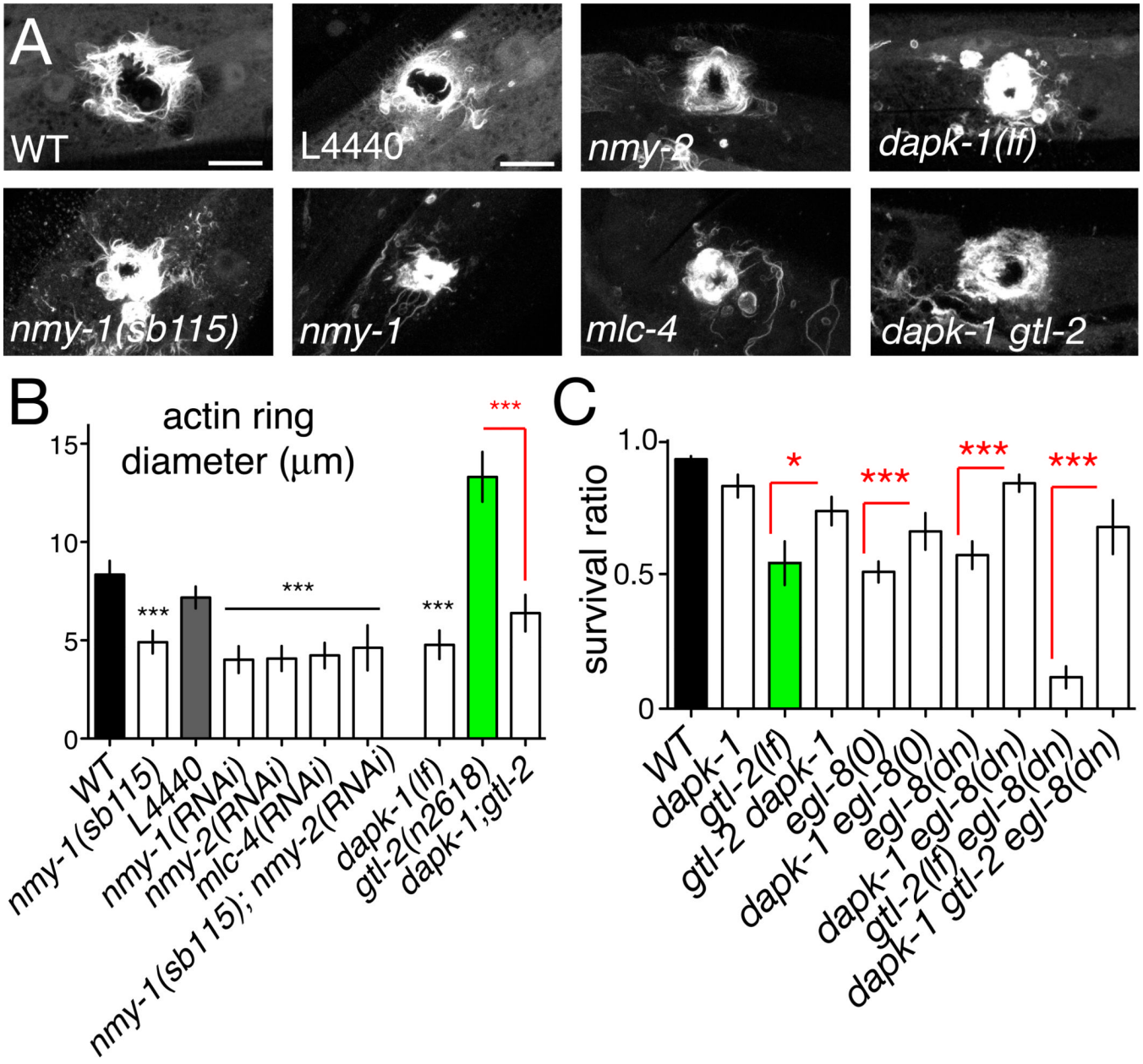

Figure 6. Negative regulation of wound closure by non-muscle myosin and DAP kinase

(A) Loss of function in non-muscle myosin and *dapk-1* promotes actin ring closure. GFP-moesin (*juIs352*) imaged at 1 h post wounding in *nmy-1(sb115)* mutants, and after RNAi for *nmy-1*, *nmy-2*, *mlc-4* (control: L4440). Survival post-wounding was unaffected under these conditions (not shown). Actin ring assembly is enhanced in *dapk-1(ju4)* and in *dapk-1 gtl-2* double mutants (compared *gtl-2* in Figure 4C). Confocal projections of *z*-stacks, 1 h post needle wound. (B) Quantitation of actin ring diameters as in Figure 4. (C) *dapk-1* suppresses the post-wound survival defects of *gtl-2*, *egl-8*, and of *gtl-2 egl-8* double mutants. n > 100 per genotype; Fisher exact test.

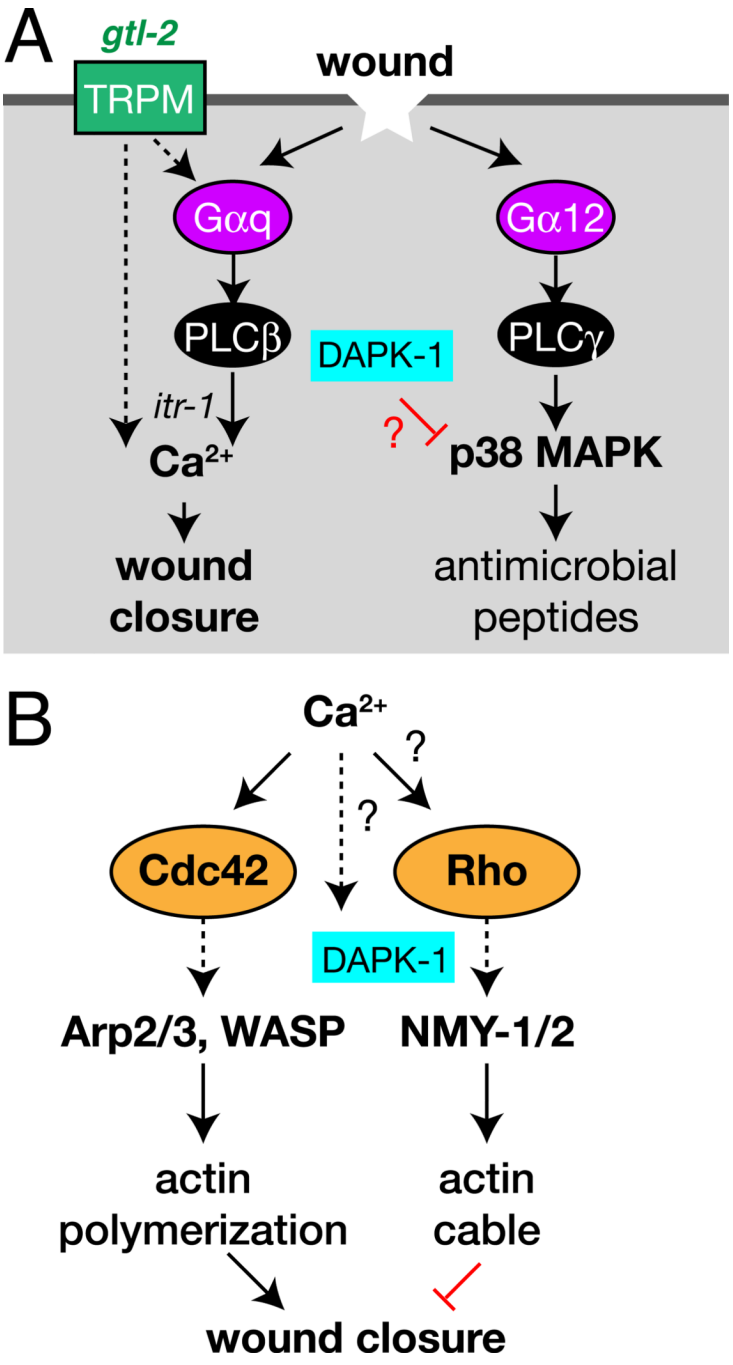

Figure 7. Wound response pathways in the adult *C. elegans* epidermis

(A) Model for the relationship of the innate immunity and wound closure pathways in *C. elegans* epidermal wound repair. (B) Possible mechanism of small GTPase regulation in wound healing.